

Do columnar defects produce bulk pinning?

M.V. Indenbom

Institute for Solid State Physics R.A.S., 142432 Chernogolovka, Moscow district, Russia

Laboratoire des Solides Irradiés, Ecole Polytechnique, 91128 Palaiseau, France

C.J. van der Beek, and M. Konczykowski

Laboratoire des Solides Irradiés, Ecole Polytechnique, 91128 Palaiseau, France

F. Holtzberg

Emeritus, IBM Thomas J. Watson Research Center, Yorktown Heights, N.Y. 10598

(February 1, 2020)

From magneto-optical imaging performed on heavy-ion irradiated $\text{YBa}_2\text{Cu}_3\text{O}_{7-\delta}$ single crystals, it is found that at fields and temperatures where strong single vortex pinning by individual irradiation-induced amorphous columnar defects is to be expected, vortex motion is limited by the nucleation of vortex kinks at the specimen surface rather than by half-loop nucleation in the bulk. In the material bulk, vortex motion occurs through (easy) kink sliding. Depinning in the bulk determines the screening current only at fields comparable to or larger than the matching field, at which the majority of moving vortices is not trapped by an ion track.

Columnar defects created by heavy ion irradiation provide very efficient vortex pinning in high temperature superconductors [1]. Nevertheless, the column radii being very homogeneous over their length [2], it is not clear how the columns can inhibit the motion of even slightly misaligned vortices. Aside from the case where the angle between the applied magnetic field and the direction of the ion beam during irradiation is deliberately chosen to be non-zero [3], misalignment between vortices and columnar defects arises from the presence of the shielding current itself, since the latter implies not only a gradient of the vortex density but also vortex line curvature. The problem is illustrated in Fig. 1. If the vortex lines are inclined with respect to the ion tracks, vortex kinks connecting segments trapped by the columns can easily slide along them. The force opposing this motion is determined by the background pinning by point defects. Hence, the critical current will be orders of magnitude lower than that corresponding to the depinning of vortices from the columns by a (double) kink nucleation process [4]. The large observed critical currents [1], as well as the moderate anisotropy for vortex motion within and across the plane containing the irradiation direction and the c -axis in obliquely irradiated $\text{DyBa}_2\text{Cu}_3\text{O}_{7-\delta}$ single crystals [3], indicates that kink sliding cannot be the main mechanism limiting flux motion type-II superconductors with correlated disorder. Rather, it was suggested [3] that, in crystals of thickness d much greater than the penetration depth λ , it is the nucleation of vortex kinks at the crystal surface that plays this role (shaded arrow in Fig. 1). By consequence, the critical current only flows in a surface layer of thickness $\sim \lambda$; kink sliding causes the current density $j(z)$ in the bulk to very rapidly decay to a value that is much too small to induce vortex-kink or half-loop nucleation.

In this paper, it is verified that vortex motion in irradiated $\text{YBa}_2\text{Cu}_3\text{O}_{7-\delta}$ (YBCO) single crystals indeed proceeds through the “hard” nucleation of kinks at the surface followed by “easy” kink sliding into the crystal bulk, *irrespective of the relative alignment between vortex lines and ion tracks*. Our method relies on the measurement of the thickness dependence of the crystals’ self-field: if the current flows only within a surface layer, the integrated shielding current $J = \int_{-d/2}^{d/2} j(z) dz$, and hence the hysteretic parts of the magnetic moment and of the induction measured at the crystal surface, should be independent of the thickness.

The most reliable way to demonstrate a thickness (in)dependence of the self-field, excluding the usual scatter of the crystal properties, is to observe the flux penetration into a flat sample with big surface steps. Supposing that the bulk current j is homogeneous, the characteristic field for penetration of perpendicular flux into a flat superconducting plate is proportional to $J = jd$ [5]; a much easier flux penetration into the thinner parts of such superconducting samples has clearly been observed using magneto-optics, and was reproduced in model

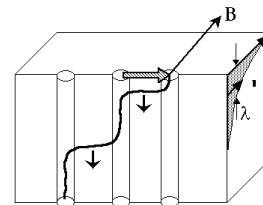


FIG. 1. Surface depinning of a vortex (bold line) from the columnar defects (cylinders). Short arrows indicate the vortex kink sliding down from the surface, producing a vortex drift to the right. The surface critical current distribution in the λ -layer is sketched on the right hand “crystal face”.

calculations [6,7]. For surface-like pinning, in which only a surface current J_s is present, $J = 2J_s$ and flux penetration should be like that into a crystal of constant thickness.

For our experiments we have selected YBCO single crystals with as-grown surface steps on one or both crystal sides, such as to have a thickness variation of at least a factor 2 over the length of the crystal. All YBCO crystals were grown in gold crucibles and annealed in oxygen in Pt tubes as described elsewhere [8]. Microscopic observations in reflected polarized light revealed all crystals to be twinned (Figs. 2(a) and 3(a,b)). The crystals were irradiated at GANIL in Caen, France, using a beam of 6 GeV Pb ions oriented parallel to the crystalline c -axis. The track density $n_d = 5 \times 10^{10} \text{ cm}^{-2}$ corresponds to the irradiation dose, and to a matching field $B_\Phi = \Phi_0 n_d = 10 \text{ kG}$ (Φ_0 is the flux quantum). Flux penetration before and after the irradiation was studied by means of the magneto-optical imaging technique using ferrimagnetic garnet indicators with in-plane anisotropy [9]. On all images of the flux distribution presented in this paper the higher value of the image intensity corresponds to the higher value of the local induction.

In Fig. 2 we present observations of the flux

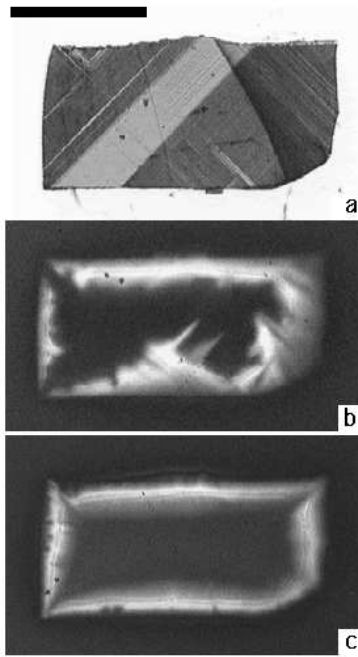


FIG. 2. Regularization of flux penetration by heavy ion irradiation: (a) Reflected polarized light photograph of the twin structure on the surface of a YBCO single crystal. The crystal has a large surface step dividing it into two parts of thickness 10 μm (RHS) and 20 μm (LHS), respectively. The length of the dark strip is 0.5 mm. (b,c) The remanent induction on the crystal surface after the application and removal of a field $H_a = 360 \text{ G} \parallel c \parallel$ ion tracks: (b) before irradiation, $T = 40 \text{ K}$; (c) after irradiation with 6 GeV Pb ions, $T = 80 \text{ K}$.

penetration into one of the crystals before and after the irradiation. The crystal has a large surface step, separating it into two parts of thickness 10 μm and 20 μm respectively. Fig. 2(b) shows the remanent induction before the irradiation, after the application and removal of an applied field $H_a = 360 \text{ G} \parallel c$ at $T = 40 \text{ K}$. Owing to the crystal's twin structure, flux penetration before the irradiation is rather irregular. This irregularity was observed in all other crystals. Nevertheless, flux penetration into the thin right hand side is clearly easier than that into the thick left hand part of the crystal.

The introduction of columnar defects drastically changes the flux penetration pattern. Because of the very substantial increase in shielding current, the temperature had to be increased to 80 K in order to observe penetration over a distance comparable to that before irradiation (Fig. 2(c)). Pinning by columnar defects is seen to dominate all other pinning: if any influence of the twin boundaries on the flux penetration is present, it can no longer be discerned [3]. More important, flux now penetrates *equally far into the thick and thin parts of the crystal* in accordance with the hypothesis of surface-like depinning.

This finding is corroborated by measurements on a specially prepared rectangular sample, cut from another irradiated crystal in order to have a series of surface steps

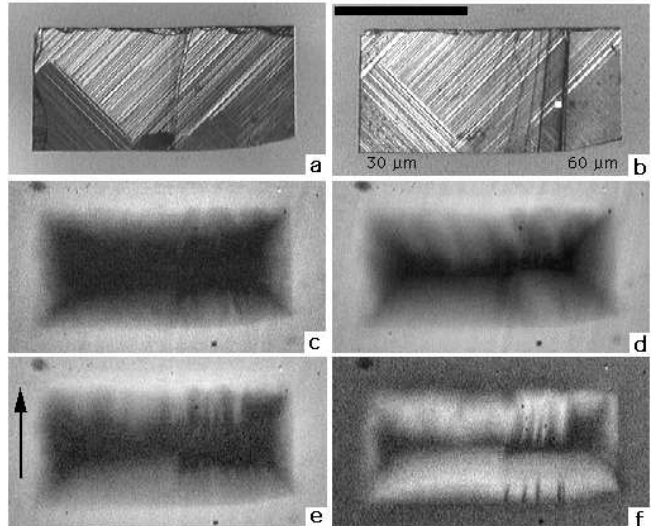


FIG. 3. Role of surface steps in the flux penetration into an YBCO crystal with columnar defects: (a) Top surface of a crystal with a 15 μm step crossing it in the center; (b) Mirror image of the bottom surface, with one large 10 μm step at the very right and a number of smaller steps. The crystal thickness monotonically increases from left to right; the dark strip has length 0.5 mm. (c,d) Homogeneous flux penetration into the ZFC crystal ($T = 85 \text{ K}$). (c) $H_a = 177 \text{ G}$, (d) $H_a = 359 \text{ G}$ ($\parallel c \parallel$ ion tracks); (e,f) Image of the perpendicular induction on the top of the crystal, cooled in a constant in-plane field $H_\parallel = 80 \text{ G}$, applied parallel to the shorter crystal sides. (e) $H_a = 169 \text{ G}$; (f) H_a reduced to 84 G after 253 G ($T = 85 \text{ K}$).

of the same sign, oriented perpendicular to its longer sides. Fig. 3(a,b) shows that this sample has a big step of height $\sim 15 \mu\text{m}$ on the top surface, dividing it into two roughly equal parts of thickness $30 \mu\text{m}$ and $50-60 \mu\text{m}$ respectively. On the bottom surface (the mirror image of which is shown in Fig. 3(b) for easier comparison with Fig. 3(a)), there is another large step of height $\sim 10 \mu\text{m}$, together with a number of smaller steps of height $\sim 1 \mu\text{m}$. The twin patterns revealed in reflected polarized light are equivalent on both crystal sides, and are not interrupted by the surface steps, thus showing the perfect continuity of the sample. Subsequent magneto-optical imaging of the flux distribution was carried out on the top surface. Again applying a field parallel to the columnar defects, *i.e.* perpendicular to the plane of the zero-field cooled sample, we observed the same striking phenomenon: the flux penetration pattern appears as if the crystal had constant thickness (Fig. 3(c,d)). The distance over which flux penetrates is the same along all the sample edges, *i.e.* J is thickness independent. Note that the small irregularities in flux penetration at the upper edge in Fig. 3(d) may be ascribed to the defects caused by cutting (seen in Fig. 3(a)).

The above result constitutes strong evidence in favor of the model in which depinning of vortices from parallel columnar defects is limited by the nucleation of vortex kinks at both crystal surfaces, the critical current being the surface current necessary for this process (Fig. 4(a)). Vortex depinning in the situation where the field is applied parallel to the columns thus resembles depinning in the case where either are misaligned [3]. Simultaneously, it is a well-known fact that the magnetic moment of heavy-ion irradiated YBCO rapidly decreases when the angle between the applied field and the columns is increased [1]. It is therefore interesting to learn how tilting the field affects surface depinning. For this, the same crystal was cooled in a field $H_{\parallel} = 80 \text{ G}$ directed parallel to the crystal plane and parallel to its shorter sides (as indicated in Fig. 3(e)). The in-plane field was not changed during the subsequent application of a perpendicular field H_{\perp} . Although the penetration of H_{\perp}

appeared to be somewhat more pronounced in the thinner left hand part of the crystal (Fig. 3(e)), the difference in penetration depth between the two parts was considerably less than what should be expected for bulk pinning, would this have been relevant after relieving the vortex confinement to the columnar defects.

We also observe an intriguing easy flux motion along the small surface steps on the bottom face of the crystal. Such a pronounced influence of these steps is not to be expected in case bulk pinning is dominant. The perpendicular induction (directed towards the observer) clearly penetrated further along the steps at the upper edge (Fig. 3(e)). When the applied field was reduced, flux left the crystal preferentially at the lower edge, while the features arising from the earlier preferential penetration at the upper edge remained frozen (Fig. 3(f)). Reversing the sign of either H_{\perp} or H_{\parallel} reversed the sense of easy flux motion along the steps: flux now penetrated preferentially at the lower edge in increasing H_{\perp} and at the upper edge in decreasing H_{\perp} .

The motion of inclined vortices is mediated by *unidirectional* kink sliding from the surface with leading vortex end, where kinks nucleate, to the opposite surface (see Fig. 4 (b)). The observed easy flux penetration along the sharp small steps on the bottom surface of the crystal is a result of easy kink nucleation at these steps. The big step on the top face is smooth and does not affect surface kink nucleation. The need to nucleate the kinks on one surface only restricts the current flow to this surface (cmf. Fig. 4), which explains the fact that inclined vortices penetrate the crystal approximately twice as far for the same temperature and H_{\perp} , as well as the rapid decrease of the sample magnetic moment when the applied field is tilted from the track direction. The strong sensitivity to surface defects is another fact supporting the idea of surface-like pinning: as in the case of the Bean-Livingston surface barrier [11] the nucleation of vortex kinks is considerably facilitated by even small but sharp surface irregularities.

Unfortunately, the magneto-optical technique is limited to low fields, at which the self-field generated by the superconductor is comparable to or larger than the applied field. In order to extend the measurements to fields comparable to B_{Φ} we used the micro Hall probe technique [10]. A small home-made single crystalline InSb Hall probe with active area $\approx 80 \times 80 \mu\text{m}^2$ was consecutively placed in equivalent positions on the thick and thin parts of the crystal shown in Fig. 3, such that in each case its distance to crystal ends was approximately equal to half the crystal width. Loops of the hysteretic induction B_H were measured for applied fields up to 50 kG and temperatures $45 \text{ K} < T < 85 \text{ K}$. Fig. 5 shows the difference $\Delta B = B_H - H_a$ measured on both the thick and the thin parts of the crystal at $T = 60$ and 80 K . The shape of these loops is in good agreement with those in the literature [1]. It is seen that the ‘local

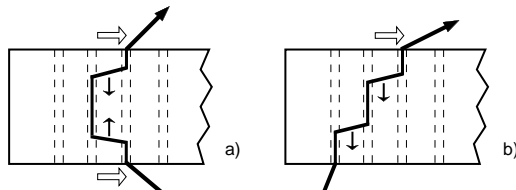


FIG. 4. Vortex kink motion in perpendicular (a) and inclined field (b): (a) Kinks nucleate at both crystal surfaces, slide into the interior and annihilate there with each other – the critical current of kink nucleation flows on the both surfaces; (b) Unipolar kinks nucleate at the vortex ‘leading head’ and move down to the opposite crystal surface – the critical current flows on the upper surface only.

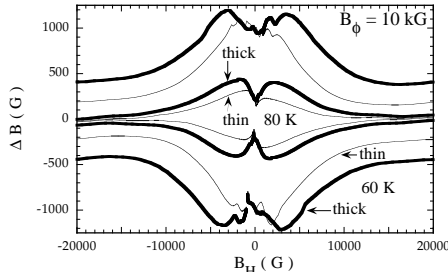


FIG. 5. “Magnetization” loops $\Delta H = B_H - H_a$, measured on the crystal shown in Fig. 3 at 60 K and 80 K. Bold lines are for the thick crystal part, thin lines represent data taken on the thin part of the crystal.

magnetization” ΔB measured on the thick and thin parts of the crystal *practically coincides* or differs by less than the amplitude of the low field ΔH irregularities ($H_a < 3$ kG and $H_a < 1$ kG for $T = 60$ K and 80 K respectively), contrary to the difference expected for ordinary bulk pinning, *i.e.* the thickness ratio ≈ 2 , and thus confirming the magneto-optical observations. This field regime, in which vortex motion is limited by kink nucleation at the surface, corresponds to the regime where the width of the magnetic hysteresis loop shows a plateau ($T \lesssim 55$ K), or increases with field ($T \gtrsim 55$ K). The loops start to deviate from each other at the field H_{max} where $|\Delta H|$ measured on the thinner part is maximum. Loops measured upon repeated cycling of the field show that H_{max} can be substantially greater than the field of full flux penetration H^* . The “magnetization” ΔH then decreases until, above $\mu_0 H_a \approx B_\Phi$, ΔH remains constant and displays the thickness dependence characteristic for bulk pinning.

We interpret the occurrence of either surface or bulk depinning in the different regimes of the magnetic hysteresis loop in terms of pinning of single vortices by individual columns at low fields (each vortex can find an empty track) and plastic vortex creep at higher fields $\gtrsim B_\Phi$. The single-vortex pinning regime corresponds to that of surface depinning. In this regime, the critical current should be estimated as $j_c \sim \Delta H/\lambda$, instead of the usual $j_c \sim \Delta H/d$. This yields a critical current value $j_c \gtrsim 10^8$ A cm⁻² for single vortex depinning from a track, which at low T tends to the initial estimates which had j_c comparable to the depairing current [12]. It is clear that with such current values, the usual critical state in the crystal bulk cannot exist: the self-field would generate large vortex curvature and many “pre-formed” vortex kinks that would immediately slide to the crystal equator and mutually annihilate. Thus bulk pinning can only appear at fields when single-vortex pinning is no longer relevant. This happens when H_a approaches a sizeable fraction of B_Φ : many free vortices appear in the system, as was directly observed by scanning tunnel microscopy [13] and revealed by model calculations [14]. In this case the plastic motion of these free vortices through the “forest” of vortices trapped by the columnar defects determines the

critical current and the screening properties of the superconductor. Although much lower than the current needed for depinning from a track, this critical current is still much higher than that of the unirradiated crystal [4,15].

In conclusion, the observed thickness independence of the shielding current in YBCO crystals with parallel columnar defects ($\parallel c$) proves that vortex depinning from the columns occurs via surface nucleation of vortex kinks which easily slide further down the columns into the sample volume. The critical current is that necessary for kink nucleation and flows only on the surface. Surface imperfections can considerably facilitate the nucleation process; sharp surface steps can induce a diode-like flow of vortices which should be seen also as an asymmetry of the magnetization loops [16]. Similar gigantic surface pinning may be expected for pinning by twin planes and for intrinsic pinning.

We gratefully acknowledge S. Bouffard for the help with the irradiation, and Th. Schuster for discussions on the central idea of the present work.

- [1] L. Civale *et al.*, Phys. Rev. Lett. **67** 648 (1991); M. Konczykowski *et al.*, Phys. Rev. B **44** 7167 (1991); V. Hardy *et al.*, Physica (Amsterdam) C **201** 85 (1992); M. Leghissa *et al.*, Europhys. Lett. **11** 323 (1992).
- [2] V. Hardy *et al.*, Nucl. Instr. and Meth. B **54**, 472 (1991); B. Holzapfel *et al.*, J. Alloys and Comp. **195**, 411 (1993).
- [3] Th. Schuster *et al.*, Phys. Rev. B **50**, 9499 (1994); Th. Schuster *et al.*, Phys. Rev. B **51**, 16358 (1995); Th. Schuster *et al.*, Phys. Rev. B **53**, 2257 (1996).
- [4] D.R. Nelson and V.M. Vinokur, Phys. Rev. Lett. **68**, 2398 (1992); Phys. Rev. B **48**, 13060 (1993).
- [5] D.J. Frankel, J. Appl. Phys. **50**, 5402 (1979); M. Daeumling and D.C. Larbalestier, Phys. Rev. B **40**, 9350 (1989); L.W. Conner and A.P. Malozemoff, Phys. Rev. B **43**, 402 (1991); E. H. Brandt and M. V. Indenbom, Phys. Rev. B **48**, 12893 (1993).
- [6] Th. Schuster *et al.*, Phys. Rev. B **50**, 16684 (1994).
- [7] Th. Schuster *et al.*, Phys. Rev. B **52**, 10375 (1995).
- [8] F. Holtzberg and C. Feild, Eur. J. Solid State Inorg. Chem. **27**, 107 (1990).
- [9] L. A. Dorosinskii *et al.*, Physica (Amsterdam) C **203**, 149 (1992); M. R. Koblischka and R. J. Wijngaarden, Supercond. Sci. Technol. **8**, 199 (1995).
- [10] M. Konczykowski, F. Holtzberg, and P. Lejay, Supercond. Sci. Technol. **4**, S331 (1991).
- [11] C.P. Bean and J.D. Livingston, Phys. Rev. Lett. **12**, 14 (1964).
- [12] E.H. Brandt, Phys. Rev. Lett. **69**, 1105 (1992).
- [13] S. Behler *et al.*, Phys. Rev. Lett. **72**, 1750 (1994).
- [14] C. Reichardt *et al.*, Phys. Rev. B **53**, R8898 (1996); C. A. Mair, Master thesis, Vrije Universiteit, Amsterdam (1998).

- [15] L. Radzihovsky, Phys. Rev. Lett. **74**, 4923 (1995); C. Wengel and U.C. Täuber, Phys. Rev. Lett. **78**, 4845 (1998).
- [16] M. Konczykowski *et al.*, Physica C **282-287**, 2189 (1997).